PHOTOELECTRON SPECTROSCOPY OF SOLVATED ANION CLUSTERS

S. T. Arnold, J. H. Hendricks, and K. H. Bowen
Department of Chemistry, Johns Hopkins University
3400 N. Charles St., Baltimore, MD 21218 USA

Abstract. The photoelectron spectra of $O^-(Ar)_{n=1-26}$ have been recorded, and total as well as sequential solvation energies have been extracted from the spectra. Plotting these values as a function of cluster size demonstrates that the first solvation shell for this system closes at n=12. Also, both the energetic data and the mass spectral data suggest structural information about the O^-Ar_n clusters. Specifically, these species appear to follow a pentagonal packing sequence, implying an icosahedral structure for n=12 and a capped icosahedral structure for n=18.

I. Introduction

Photodetachment studies of solvated anion clusters began in 1968, with the threshold photodetachment study of $OH^-(H_2O)$ by Golub and Steiner.[1] In 1985, we applied negative ion photoelectron (photodetachment) spectroscopy to the study of solvated anion clusters,[2] and this technique has proven to be very useful in examining the energetics of these cluster anions. Since then, we have applied negative ion photoelectron spectroscopy to the study of $H^-(NH_3)_{n=1-2}$, $NH_2^-(NH_3)_{n=1-2}$, $NO^-(N_2O)_{n=1-5}$, $NO^-(H_2O)_{n=1-2}$, and $NO^-(Rg)$, where Rg = Ar, Kr, and Xe;[3-6] Miller, Leopold, and Lineberger[7] have investigated $H^-(H_2O)$; Johnson et al.[8,9] have studied $O_2^-(O_2)$, $O_2^-(N_2)$, and $(NO)_2^-$; and recently Cheshnovsky and coworkers[10] have studied $I^-(H_2O)_{n=1-15}$, while Neumark and coworkers[11] have examined $I^-(CO_2)_{n=1-13}$. Also very relevant to anion solvation are the photodissociation studies of $Br_2^-(CO_2)_{n=1-24}$ and $I_2^-(CO_2)_{n=1-22}$ by Lineberger and coworkers.[12,13] Here, continuing our photoelectron studies of solvated anion clusters, we present the photoelectron spectra of $O^-(Ar)_{n=1-26}$. This particular solvated anion system was chosen for study because of its relative simplicity, an atomic anion interacting with rare gas solvent atoms, providing a system in which all the components are spherical and in which solvent-solvent interactions are minimized.

J. Jortner et al. (eds.), Reaction Dynamics in Clusters and Condensed Phases, 37–45.

II. Experimental

Negative ion photoelectron spectroscopy is conducted by crossing a mass selected beam of negative ions with a fixed-frequency photon beam and energy analyzing the resultant photodetached electrons. Our negative ion photoelectron spectrometer has been previously described in detail.[14] A supersonic expansion source coupled with an additional gas "pickup" line was used to generate the O^-Ar_n cluster anions. Typically, 8-10 atm of argon was expanded through a 12 μm nozzle into vacuum, while a small amount of N_2O was introduced into the plasma through a secondary "pick-up" line located just beyond the nozzle. A cooling jacket around the stagnation chamber allowed the source temperature to be maintained at -70 °C. A negatively biased filament (ThO_2/Ir) was used for ionization, forming O^- and NO^- anions, which then clustered with the argon in the expansion, forming O^-Ar_n and NO^-Ar_n as the primary cluster anions. A predominantly axial magnetic field confined the plasma and enhanced cluster anion production. Cluster anions were extracted into the spectrometer and transported through a Wien velocity selector, where they were mass selected. As shown in Figure 1, "magic numbers" were observed in the mass spectrum of O^-Ar_n, where n=10,12,15,18,22, and 25 were more intense than their neighboring clusters. The mass selected cluster ion beam was then crossed with an Ar^+ laser operated intracavity (488 nm or 457.9 nm), and the resulting photodetached electrons were energy analyzed using a hemispherical electron energy analyzer, with a typical resolution of 35 meV.

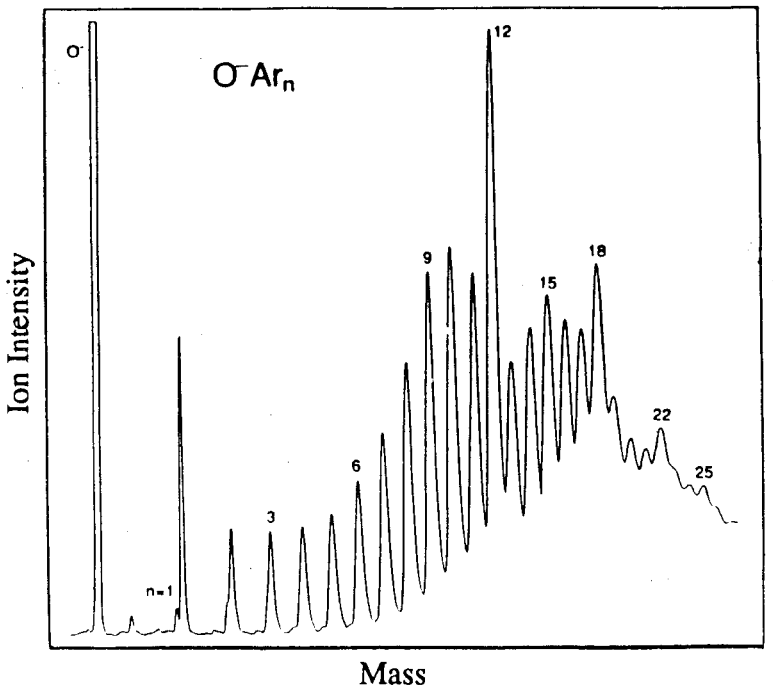

Figure 1. In the mass spectrum of O^-Ar_n, "magic numbers" were observed at n=10,12,15,18,22, and 25.

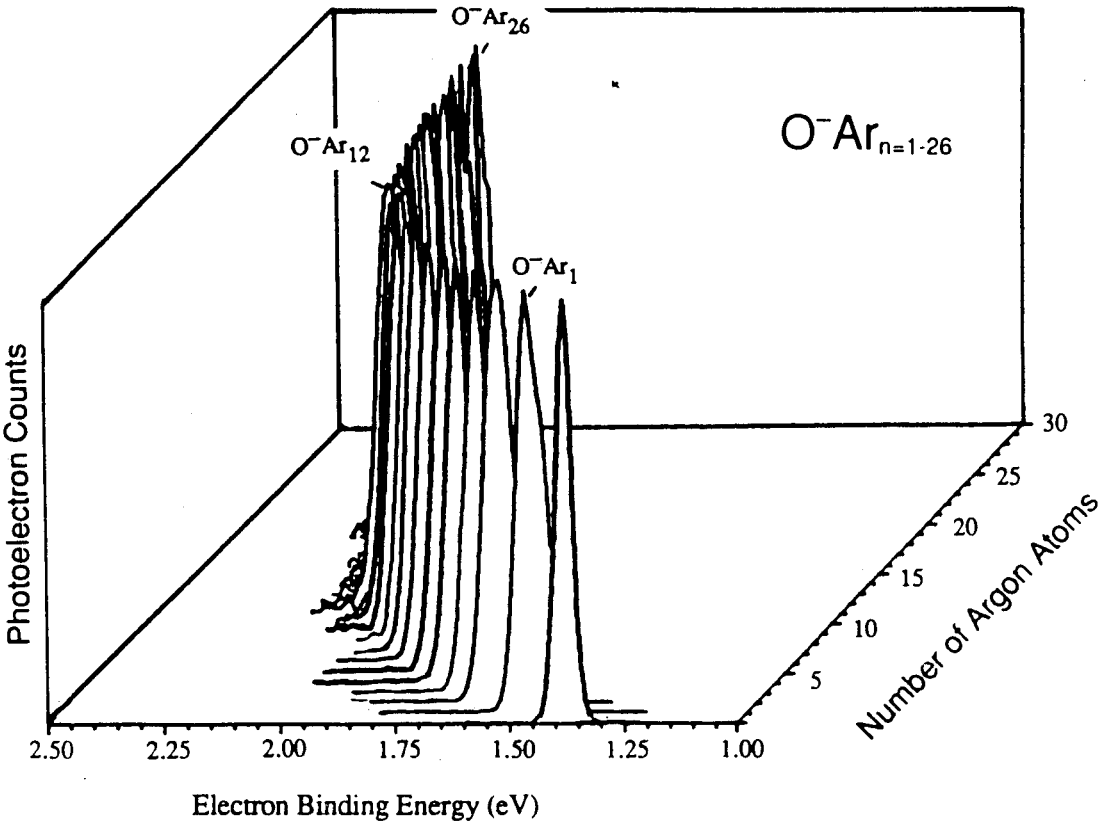

Figure 2. The negative ion photoelectron spectra of $O^-(Ar)_{n=1-26}$. All the spectra closely resemble that of O^-, each containing a single peak which shifts to higher electron binding energy with increasing cluster size. The electron binding energy at the peak maximum is the VDE of the anion.

III. Photoelectron Spectra

The negative ion photoelectron spectra of $O^-(Ar)_{n=1-26}$ are presented in Figure 2, along with the photoelectron spectrum of O^-, which was recorded before and after each cluster anion spectrum for calibration purposes. The photoelectron spectrum of O^- appears as a single, slightly broadened peak. Because O^- serves as the "chromophore" for photodetachment in O^-Ar_n, the cluster anion spectra each closely resemble that of O^-, except for being broadened and shifted toward higher electron binding energy with increasing cluster size. The electron binding energy at the peak maximum in each case is the vertical detachment energy (VDE) of the anion. This is the vertical photodetachment transition energy between the ground state of the anion and the ground state of the neutral at the equilibrium geometry of the negative ion.

IV. Cluster Anion Energetics

The energetics of the O^-Ar_n clusters are governed by the following relationship:

$$EA[O(Ar)_n] = EA[O] + \sum_{m=0}^{n-1} D_0[O^-(Ar)_m\cdots Ar] - \sum_{m=0}^{n-1} D_0[O(Ar)_m\cdots Ar] \quad (1)$$

where EA denotes the adiabatic electron affinity, $D_0[O^-(Ar)_m\cdots Ar]$ is the ion-neutral dissociation energy for the loss of a single Ar atom from the cluster, and $D_0[O(Ar)_m\cdots Ar]$ is the analogous neutral cluster weak-bond dissociation energy for the loss of a single Ar atom. Since ion-solvent interaction energies generally exceed van der Waals bond strengths, it is evident from eq (1) that clustering can be expected to stabilize the excess electronic charge on a negative ion, ie. the electron affinities of these clusters should increase with cluster size. This is seen in the photoelectron spectra of O^-Ar_n, where the sub-ion is stabilized as the number of solvent atoms increases, shifting the spectra toward higher electron binding energies. It follows from eq (1), that the relationship between adjacent-sized clusters can be expressed as:

$$EA[O(Ar)_n] - EA[O(Ar)_{n-1}] = D_0[O^-(Ar)_{n-1}\cdots Ar] - D_0[O(Ar)_{n-1}\cdots Ar] \quad (2)$$

Although these equations describe the cluster anion energetics rigorously, some approximations may be made to further simplify these expressions. The EA of each cluster can be approximated by the VDE of the O^-Ar_n anion. The VDE of O^- (1.465 eV) nearly equals the EA (1.462 eV), and because O^- serves as the photodetachment chromophore for the O^-Ar_n cluster anions, the EA of the cluster is taken to be nearly equal to the measured cluster anion VDE. In addition, ion-solvent interaction energies are often larger than van der Waals energies by an order of magnitude, so their relatively minor contributions in eqs (1) and (2) may be neglected. Thus, the total anion-solvent dissociation energy for a given cluster anion may be approximated as the difference between the VDE of that species and the VDE of the sub-ion:

$$\sum_{m=0}^{n-1} D_0[O^-(Ar)_m\cdots Ar] \approx VDE[O^-(Ar)_n] - VDE[O^-] \quad (3a)$$

while cluster ion-single solvent dissociation energies for O^-Ar_n may be approximated by the difference between the VDEs of two adjacent-sized clusters:

$$D_0[O^-(Ar)_{n-1}\cdots Ar] \approx VDE[O^-(Ar)_n] - VDE[O^-(Ar)_{n-1}] \quad (3b)$$

This is equivalent to saying that the spectral shift from that of O^- is an approximation to the total anion solvent dissociation energy, while the spectral shift between adjacent-sized cluster ions is an approximation to that particular anion-single solvent dissociation energy.

The approximation to neglect the neutral weak bond dissociation energy can be justified by examining the energetics of $O^-(Ar)_1$. Because there is information available about the neutral dissociation energy of O(Ar),[15] the dissociation energy of $O^-(Ar)$ can be

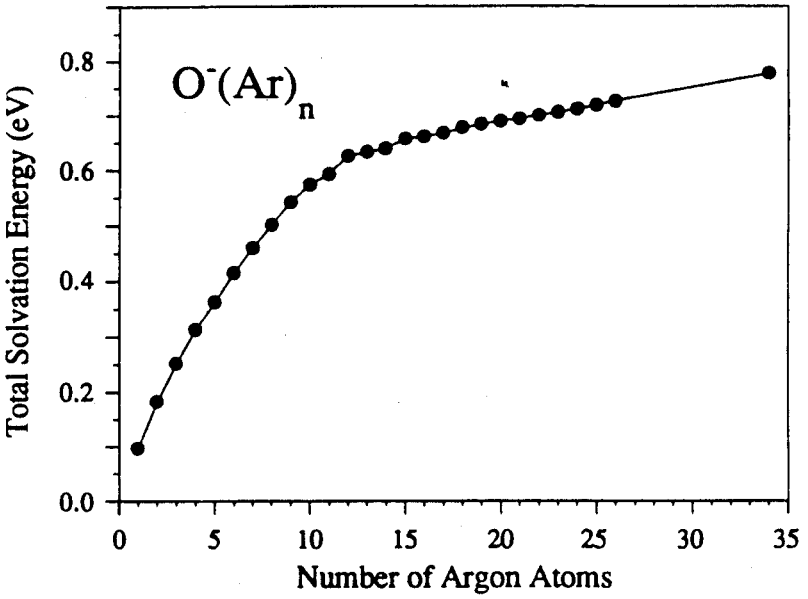

Figure 3. The total anion-solvent dissociation energy of $O^-Ar_{n=1-26}$ plotted as a function of cluster size. Preliminary data for n=34 is also included on the plot. The dramatic change in the slope at n=12 is consistent with the closing of the first solvation shell.

determined from eq(1). The vibrational frequency for the ground state of O(Ar) is ~20 cm^{-1} and D_e[O···Ar] is 0.010 eV, so the neutral dissociation energy D_0[O···Ar] is 0.009 eV. In addition, the observed VDE of O^- is nearly equal to the EA of O, and this is expected for O^-Ar as well, so EA[O(Ar)] ≈ VDE[O^-(Ar)] and EA[O] ≈ VDE[O^-]. This leads to an anion-solvent dissociation energy D_0[O^-···Ar] of 0.106 eV. Thus, the anion dissociation energy (D_0[O^-···Ar]) is greater than that of the neutral (D_0[O···Ar]) by an order of magnitude. The dissociation energy for O^-(Ar), determined from eq(3) is 0.097 eV, which is slightly less than the value given from eq(1).

V. Interpretation

A. Solvation Shell Closing

The total anion solvent dissociation energy is the total amount of energy the oxygen sub-ion is stabilized by its association with a given number of argon atoms. This total solvation energy, shown as a function of cluster size for the O^-Ar_n system in Figure 3, increases smoothly up to n=12, where it changes slope. While the average stabilization energy per atom remains relatively large for n<12, it decreases significantly and remains relatively constant for n=13-26. The dramatic change in the slope of this plot at n=12 indicates a major change in the interaction of subsequent argon atoms with the cluster ion,

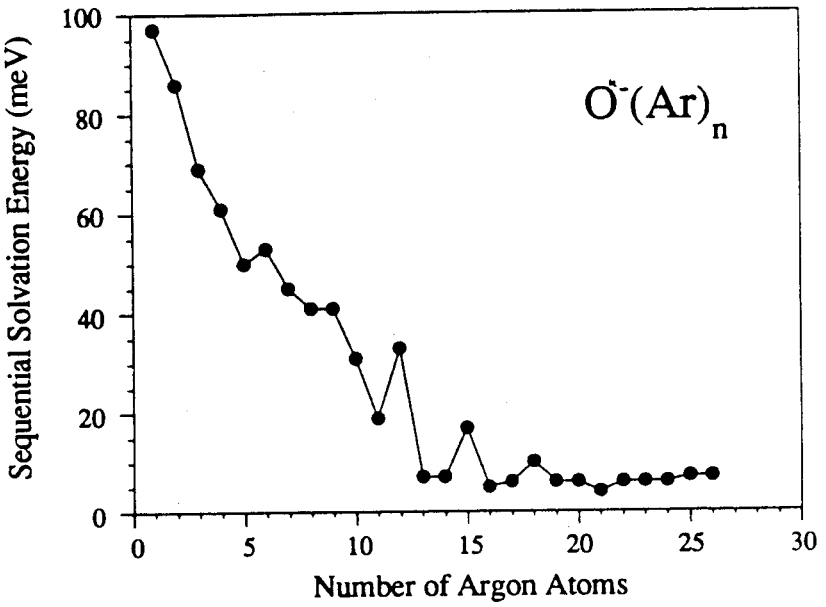

Figure 4. The sequential solvation energies of O^-Ar_n as a function of cluster size. Discontinuities in this plot at n=6,9,12,15, and 18 suggest structural information about these cluster anions. (An error bar of ± 5 meV is typical for the data.)

and it is consistent with the first solvation shell closing around the O^- sub-ion with 12 argon atoms. The decrease in the average stabilization energy for n>12 is a result of the additional argon atoms being shielded from the O^- sub-ion. As is further shown below, the first solvation shell closes at O^-Ar_{12}, as the O^- sub-ion is completely enclosed in a cage of argon solvents.

B. Cluster Structure

Additional structural implications for the O^-Ar_n system emerge upon examining cluster anion-single solvent dissociation energies as a function of cluster size. These dissociation energies are essentially stepwise (sequential) solvation energies because they quantify the effect each additional individual argon solvent has on the stability of the O^-Ar_n cluster. The interaction between O^- and the first few argon solvents is expected to be the strongest, while the stabilizing effect of each additional solvent should diminish as the cluster grows and the sub-ion's localized charge interacts with a greater number of solvent atoms. In the absence of structural effects, this should lead to a monotonically decreasing function of stepwise solvation energies with increasing cluster size.

The stepwise solvation energies for O^-Ar_n are shown in Figure 4 as a function of cluster size, and they follow the expected generally decreasing trend. However, discontinuities in this decreasing trend are observed at n=6,9,12,15, and 18, indicating that these particular clusters are being stabilized by some additional effect. The largest single discontinuity in the stepwise solvation energy trend occurs at n=12, and this is

followed by an abrupt drop in sequential solvation energy at n=13. We interpret this as further evidence for the first solvation shell closing at n=12. The small sequential solvation energies for n=13 and n=14 are consistent with the sub-ion being shielded, resulting in weaker ion-neutral interactions.

The additional stability observed for the 12th argon atom is consistent with the cluster having an energetically favorable structure, which is likely to occur at a solvation shell closing. The mass spectrum presented earlier demonstrates that n=12 is the primary magic number observed, and while it may be misleading to suggest structural implications based on mass spectral magic numbers alone, it seems likely from the energetic data, as well as from the mass spectrum, that n=12 is forming an especially stable cluster anion. This suggests that the discontinuities in the sequential solvation energy plot at n=6,9,15, and 18 may also occur because of structural reasons. The mass spectrum at least partially supports this notion, with magic numbers occurring at n=10,12,15,18,22, and 25.

To better understand the structural implications of the sequential solvation energy plot (Figure 4), it is useful to examine the packing schemes that have been proposed in the past for the clustering of rare gas atoms. In particular, minimum energy structures for rare gas clusters of sizes n=6-60 were examined by Hoare and Pal using hard-sphere potentials, and three different packing sequences were found to compete: tetrahedral, pentagonal, and icosahedral.[16] For the size range of clusters we have examined here, ie. n<26, the pentagonal growth sequence consistently yielded the lowest energy structures. In this packing sequence, there are several particularly stable geometries which posses complete D_{5h} symmetry. These are the pentagonal bipyramid structure for the 7 atom cluster (which serves as the building block for larger clusters in this sequence), the icosahedral structure for the 13 atom cluster, and the capped (double) icosahedral structure for the 19 atom cluster. The tetrahedral sequence, on the other hand, predicts particularly stable structures for the 4, 8, 14, and 26 atom clusters, while the icosahedral sequence begins with the 13 atom icosahedron and predicts particularly stable structures for the 33 and 45 atom clusters (both of which are out of our size range). For larger clusters, n>26, these three sequences compete to give a variety of stable structures.

Sphere packing sequences such as these have been used to interpret the mass spectrum of Xe_m^+, which exhibits magic numbers at m=13,16,19,23,25,55,71,87, and 147.[17] A sequence of full shell icosahedra are expected for m=13,55, and 147. Adding one and two caps of 6 atoms each to m=13 yields m=19 and m=25, and adding one and two caps of 16 atoms each to m=55 yields m=71 and m=87, largely explaining the observed size distribution.

The "magic numbers" observed in the mass spectrum of O^-Ar_n are n=10,12,15,18,22, and 25, which correspond to clusters of 11,13,16,19,23, and 26 total atoms. This sequence of magic numbers is very similar to the observed pattern for Xe_m^+ clusters in the same size range, suggesting these two systems have similar structures. Moreover, the discontinuities observed in the stepwise solvation energy vs cluster size plot (Figure 4) for O^-Ar_n are n=6,9,12,15, and 18, which correspond to clusters with 7,10,13,16, and 19 total atoms. This observed sequence of 7,13, and 19 suggests that these cluster ions are following the pentagonal packing pattern described above. The intermediate magic numbers at 10 and 16 total atoms are probably due to the formation of

partially capped structures (Adding a cap of 3 atoms to (n+1)=7 and (n+1)=13 yields (n+1)=10 and (n+1)=16, respectively).

For the case of O^-Ar_{12}, the evidence implies that this cluster has an icosahedral structure. Evidence for O^- being inside the cluster rather than on the surface comes from the dramatic drop in the stepwise solvation energy at n=13. If the ion were to reside on the surface of the cluster, the sequential solvation energy for n=12 and n=13 would be comparable. However, we observe a large drop in the sequential solvation energy at n=13, which is consistent with the 13^{th} argon being shielded from the O^- core. Geometrical arguments also demonstrate that the O^- anion can fit into a cavity formed by 12 argon atoms given that the ionic radius of O^- is ~1.7 Å ,[18] the atomic radius of Ar is ~1.2 Å,[18] and the Ar-Ar bond is longer than the O-Ar bond.[15]

The evidence suggests that O^-Ar_n structures resemble those of pure rare gas clusters and that they follow the pentagonal packing sequence with O^-Ar_{12} as an icosahedron, O^-Ar_{15} as a partially capped icosahedron, and O^-Ar_{18} as a fully capped (double) icosahedron. The packing of atoms in accord with a packing sequence for spheres implies the domination of repulsive forces in these systems. However, since one of the components in the clusters in an ion, attractive forces must also play an important role. The competition between attractive and repulsive forces in O^-Ar_n, along with its structural implications, will be explored in a subsequent publication.

Acknowledgements. We gratefully acknowledge the support of the US National Science Foundation under Grant CHE-9007445.

References

1. Golub, S. and Steiner, B. (1968) "Photodetachment of $[OH(H_2O)]^-$", J. Chem. Phys. **49**, 5191-5193.
2. Coe, J.V., Snodgrass, J.T., Freidhoff, C.B., McHugh, K.M., and K.H. Bowen (1985) "Negative ion photoelectron spectroscopy of the negative cluster ion $H^-(NH_3)$", J. Chem. Phys. **83**, 3169-3170.
3. Coe, J.V., Snodgrass, J.T., Freidhoff, C.B., McHugh, K.M., and K.H. Bowen (1987) "Photoelectron spectroscopy of the negative cluster ions $NO^-(N_2O)_{n=1-2}$", J. Chem. Phys. **87**, 4302-4309.
4. Snodgrass, J.T., Coe, J.V., Freidhoff, C.B., McHugh, K.M., and K.H. Bowen (1988) "Photodetachment spectroscopy of cluster anions. Photoelectron spectroscopy of $H^-(NH_3)_1$, $H^-(NH_3)_2$, and the tetrahedral isomer of NH_4^-", Faraday Discuss. Chem. Soc. **86**, 241-256.
5. Bowen, K.H. and Eaton, J.G. (1988) "Photodetachment spectroscopy of negative cluster ions", in R. Naaman and Z. Vager (eds.), The Structure of Small Molecules and Ions, Plenum Publishing, pp. 147-169.
6. Eaton, J.G., Arnold, S.T., and Bowen, K.H. (1990) "The negative ion photoelectron (photodetachment) spectra of $NO^-(H_2O)_{n=1-2}$", Int. J. of Mass Spectrom. and Ion Proc. **102**, 303-312.

7. Miller, T.M., Leopold, D.G., Murray, K.K., and Lineberger, W.C. (1985) Bull. Am. Phys. Soc. **30**, 880.

8. Posey, L.A., Deluca, M.J., and Johnson, M.A. (1986) "Demonstration of a pulsed photoelectron spectrometer on mass-selected negative ions: O^-, O_2^-, and O_4^-", Chem. Phys. Lett. **131**, 170-174.

9. Posey, L.A., and Johnson, M.A. (1988) "Pulsed photoelectron spectroscopy of negative cluster ions: isolation of three distinguishable forms of $N_2O_2^-$", J. Chem. Phys. **88**, 5383-5395.

10. Markovich, G., Giniger, R., Levin, M., and Cheshnovsky, O. (1991) "Photoelectron spectroscopy of iodine anion solvated in water clusters", J. Chem. Phys. **95**, 9416-9419.

11. Arnold, D.W., Bradforth, S.E., Kim, E.H., and Neumark, D.M. (1992) "Anion photoelectron spectroscopy of iodine-carbon dioxide clusters", J. Chem. Phys. **97**, 9468-9471.

12. Alexander, M.L., Levinger, N.E., Johnson, M.A., Ray, D., Lineberger, W.C. (1988) "Recombination of Br_2^- photodissociated within mass selected ionic clusters", J. Chem. Phys. **88**, 6200-6210.

13. Papanikolas, J.M., Gord, J.R., Levinger, N.E., Ray, D., Vorsa, V., and Lineberger, W.C. (1991) "Photodissociation and geminate recombination dynamics of I_2^- in mass-selected $I_2^-(CO_2)$ cluster ions", J. Phys. Chem. **95**, 8028-8040.

14. Coe, J.V., Snodgrass, J.T., Freidhoff, C.B., McHugh, K.M., and Bowen, K.H. (1986) "Photoelectron spectroscopy of the negative ion SeO^-", J. Chem. Phys. **84**, 618-625.

15. Huber, K.P. and Herzberg, G. (1979) Constants of Diatomic Molecules, Van Nostrand Reinhold Company, New York, pp. 32-36.

16. Hoare, M.R. and Pal, P.(1971) "Physical cluster mechanics: statics and energy surfaces for monatomic systems", Adv. Phys. **20**, 161-196.

17. Recknagel, E (1984) "Production and properties of atomic and molecular microclusters", Ber. Bunsenges. Phys. Chem. **88**, 201-206.

18. Weast, R.C., Astle, M.J., and Bayer, W.H. (eds.) (1986) CRC Handbook of Chemistry and Physics, vol. 66, CRC Press, Boca Raton, Florida, p. E67, p. F164.